Cement & Concrete Composites 31 (2009) 176–185

Contents lists available at ScienceDirect

Cement & Concrete Composites

journal homepage: www.elsevier.com/locate/cemconcomp

Analysis of calcium leaching behavior of plain and modified cement pastes in pure water

Jitendra Jain, Narayanan Neithalath *

Department of Civil and Environmental Engineering, Clarkson University, Potsdam, NY 13699, United States

ARTICLE INFO

Article history:
Received 25 August 2008
Received in revised form 6 January 2009
Accepted 7 January 2009
Available online 10 January 2009

Keywords:
Leaching
Cement pastes
Porosity
Calcium hydroxide
C–S–H
Calcium ions
Equilibrium curves
Leaching depth

ABSTRACT

The calcium ion leaching behavior of cement pastes modified with a high-alkali fine glass powder, silica fume, and fly ash, exposed to deionized water, is reported in this paper. Porosity enhancement in pastes subjected to leaching is attributed both to the dissolution of calcium hydroxide (CH) as well as decalcification of C–S–H gel. A methodology that combines the measured porosity increase along with the CH and C–S–H contents remaining after leaching for a particular duration is developed to separate the porosities created due to CH and C–S–H leaching. In order to quantify the influence of leaching on the amounts of Ca ions remaining in the CH and C–S–H phases, solid–liquid equilibrium curves for calcium are developed for the unleached and leached pastes. Leaching depths are also calculated using the CH contents of the leached and unleached specimens. All the modified pastes show better leaching resistance than the plain paste. In addition to the microstructure densification, the lower Ca–Si molar ratio in modified pastes that reduces the equilibrium liquid Ca ion concentration contributes to this observation. For the glass powder modified paste, the presence of higher alkali content in the pore solution further reduces the dissolution of CH due to common ion effect, thus providing it with the highest leaching resistance. Fly ash and silica fume modified pastes demonstrate leaching resistance in between those of the plain and glass powder modified mixtures.

1. Introduction

Leaching of calcium ions from cement paste matrix is of concern in concrete structures used for radioactive waste disposal, and underground and underwater members that are constantly exposed to low pH environment. Pure or deionized water is one of the strong decalcifying agents of cement based materials [1–3]. Leaching is a combined diffusion–dissolution/precipitation process. The concentration gradients between the pore solution and the pure water cause diffusion of calcium ions from the pore solution to the surrounding ion free water. The reduction in concentration of calcium ions in the pore solution forces the dissolution of calcium hydroxide (CH) and calcium–silicate–hydrate (C–S–H) gel [3–6]. This results in increased material porosity, and consequently increased permeability, and reduced mechanical properties [7–9]. The influence of porosity on leaching, and the changes induced in the pore structure because of leaching are detailed in [10,11]. Models to explain the degradation kinetics and property changes due to leaching either individually or in combination with other chemical processes have been reported [12–15].

The use of silica fume or fly ash as supplementary cementing materials is reported to result in reduced calcium leaching [16,17]. A recent study [18] has investigated the use of silica nanoparticles to control calcium leaching in cement pastes. Apart from the pozzolanic reaction of nano-silica that reduces the porosity, this study showed that nano-silica modifies the internal structure of the C–S–H gel by increasing the average length of silicate chains, which increases calcium stabilization. Increase in silicate anion chain length of C–S–H gel with increase in dissolution (or reduction in Ca–Si molar ratio of the solid phase) has also been reported in [19]. Some studies [5,20,21] have reported that C–S–H gel begins to dissolve only after complete dissolution of CH, i.e., dissolution reactions do not occur concurrently. However, other authors [19,22] have reported that CH does not have to dissolve completely for C–S–H dissolution to occur, and this is a function of the mass (or volume) ratios of the leachant to the solid. For lower liquid-to-paste mass or volume ratios CH preferentially dissolves, while both CH and C–S–H dissociation are reported to occur in powdered samples of pastes for liquid-to-paste mass ratios (m_L/m_P) higher than 500 [19]. This value will change with surface-to-volume ratios of the sample. The solubility product of the C–S–H gel is also a function of Ca–Si ratio of the gel [23,24].

This paper investigates the influence of two high silica cement replacement materials – a fine glass powder (72.4% SiO_2) and silica fume (93.4% SiO_2) – on the leaching resistance of cement pastes exposed to deionized water and compares the performance of these modified pastes to a plain paste and a fly ash modified paste.

* Corresponding author. Tel.: +1 315 268 1261; fax: +1 315 268 7985.
E-mail address: nneithal@clarkson.edu (N. Neithalath).

0958-9465/$ - see front matter © 2009 Elsevier Ltd. All rights reserved.
doi:10.1016/j.cemconcomp.2009.01.003

Table 1
Chemical composition and physical characteristics of the materials used.

Composition (% by mass)/property	Cement	Fine glass powder (GP)	Fly ash (FA)	Silica fume (SF)
Silica (SiO_2)	20.2	72.5	50.24	93.4
Alumina (Al_2O_3)	4.7	0.4	28.78	0.42
Iron oxide (Fe_2O_3)	3	0.2	5.72	0.52
Calcium oxide (CaO)	61.9	9.7	5.86	1.91
Magnesium oxide (MgO)	2.6	3.3	1.74	–
Sodium oxide (NaO)	0.19	13.7	0.96[a]	0.25
Potassium oxide (K_2O)	0.82	0.1		0.79
Sulfur trioxide (SO_3)	3.9	–	0.51	0.34
Loss on ignition	1.9	0.36	2.8	2.3
Median particle size (μm)	13	20	20	<1
Density (kg/m^3)	3150	2490	2250	2200

[a] Equivalent alkalis.

Porosity measurements and thermogravimetric analysis are conducted on unleached and leached specimens. The Ca ion content in CH and C–S–H phases before and after leaching are quantified using equilibrium curves for calcium. Indirect estimation of leaching depths from thermal analysis results is also reported.

2. Experimental program

2.1. Materials and mixtures

Type I/II ordinary Portland cement conforming to ASTM C 150 was used for all the mixtures described in this study. A Class F fly ash (FA) conforming to ASTM C 618, a dry densified silica fume (SF), and a fine glass powder (GP) were used as partial cement replacement materials. Several replacement levels of these supplementary cementing materials were studied, but in order to keep the discussions succinct, only the results for 10% replacement of cement by mass with fly ash and glass powder, and 6% replacement of cement by mass with silica fume (referred to as GP10, FA10, and SF6, respectively, in the graphs) will be discussed in this paper. The chemical composition and physical characteristics of materials used are given in Table 1. It can be seen that the median particle sizes of glass powder and fly ash are similar, and higher than that of the cement. All the pastes were prepared with a water-to-cementing materials ratio (w/cm) of 0.40.

The cement pastes were cast in prismatic molds of size 150 mm × 50 mm × 25 mm, and cured in saturated limewater for 90 days to facilitate hydration of cement and the replacement materials. After the curing duration, prismatic pieces of size 15 mm × 10 mm × 5 mm were cut from the larger specimens, and immersed in deionized water for leaching. The leaching tests were carried out in sealed containers filled with deionized water from which CO_2 was removed. A m_L/m_p of 1000 was used, and the leachant was not renewed during the duration of the tests.

2.2. Test methods

The unleached specimens (cured for 90 days), as well as those leached in deionized water for 28, 56, or 90 days, were subjected to porosity measurements as per the procedure described in [25]. The 15 mm × 10 mm × 5 mm size specimens were removed from the containers, surface-dried, and kept in an oven at 105 °C for 24 h. After cooling to room temperature, the initial masses (m_1) of the specimens were determined. The specimens were then vacuum dried for 3 h, after which they were saturated under vacuum for another hour, and left to soak in water for 18 h. The masses of saturated surface-dried specimens (m_2) were recorded. The difference between these masses was expressed as a percent of initial mass, then converted into a percent of the initial volume of the specimen, and reported as the porosity.

The unleached and leached specimens were subjected to thermogravimetric analysis (TGA) to determine the CH and C–S–H contents in the specimens. TGA was carried out before and after 28 and 90 days of exposure to deionized water. Any portion of the unleached specimen can be expected to provide the actual CH and C–S–H contents of the pastes in that state. However, in order to obtain the residual CH and C–S–H contents in leached specimens, a representative portion containing both the leached and unleached zones need to be used for TGA. This is accomplished by removing a 6 mm × 10 mm × 5 mm section of the leached specimen as shown in Fig. 1. Five sides of this representative zone are subjected to leaching, and the ratio of the total area of the leached surfaces to the volume of the representative zone is 0.76 mm^{-1}. For the entire specimen, though the leaching is from all six sides, the corresponding ratio is very similar (0.73 mm^{-1}). Similarly, if a leaching depth of 1 mm is assumed uniformly from all sides of the specimen, the ratio of the unleached volume to the total volume of the 15 mm × 10 mm × 5 mm specimen is 0.416. For the representative zone where leaching occurs in five of the six sides, the ratio of the unleached volume to the volume of the representative zone is 0.40. Therefore, from considerations of the surface area to volume ratios, and the unleached to leached volume ratios, the sectioned zone can be considered to be representative of the entire leached sample.

The powdered sample was heated from room temperature up to 1050 °C at the rate of 10 °C per min in a Perkin–Elmer thermogravimetric analyzer. The mass drop in the thermogravimetric curve at temperatures between 400 and 450 °C indicates loss of water from CH. The amount of CH in the specimen (in terms of percentage of mass of the sample at 105 °C) is calculated directly from the thermogravimetric curves using the following equation:

$$\mathrm{CH}\ (\%) = \mathrm{WL_{CH}}\ (\%) \times \frac{\mathrm{MW_{CH}}}{\mathrm{MW_H}} \tag{1}$$

where WL_{CH} corresponds to the mass loss in percentage attributable to CH dehydration, and MW_{CH} and MW_H are the molecular weights of CH and water, respectively.

Different temperature ranges in a thermogravimetric curve are reported to indicate the water loss from C–S–H gel. Previous studies have suggested temperature ranges of 180–300 °C [26], 200–400 °C [27], and from 105 °C until the water loss corresponding to CH dehydration [22]. In this study, the mass loss between 150 °C and the temperature at which CH loss begins (~400 °C) is considered to indicate the loss of water from C–S–H gel. The amount of C–S–H is calculated as:

$$\mathrm{CSH}\ (\%) = \mathrm{WL_{CSH}}\ (\%) \times \frac{\mathrm{MW_{CSH}}}{2.1 * \mathrm{MW_H}} \tag{2}$$

where WL_{CSH} corresponds to the mass loss in percentage that occurs during C–S–H dehydration, and MW_{CSH} and MW_H are the molecular

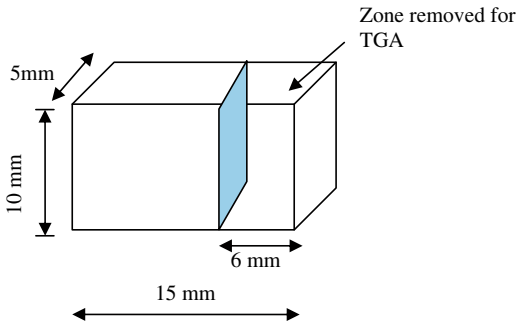

Fig. 1. Geometry of the specimen subjected to leaching, and the representative zone used for thermal analysis.

weights of C–S–H and water, respectively. Even though the chemical formula of C–S–H is taken as $C_{1.7}SH_4$, some part of the 4 moles of water will be removed at temperatures below 150 °C. The equilibrium composition of C–S–H is thus taken as $C_{1.7}SH_{2.1}$ as given in [22], which explains the division by 2.1 used in Eq. (2).

3. Results and discussions

3.1. Influence of leaching on the porosity and diffusion coefficients of pastes

Fig. 2 shows the total porosity (ϕ_T) of the cement pastes cured in saturated limewater for 90 days, and those leached for 28, 56, or 90 days in deionized water. The porosity of cement pastes depend on w/cm, degree of hydration, presence of cement replacement materials, and their reactivity. Since cement replacements by the supplementary materials have been carried out in this study on a mass basis, the initial porosity (at very early ages) of the modified pastes will be lower than that of the plain paste, because of the lower specific gravities of the replacement material than the cement it replaces. However, as cement hydration progresses, the plain paste will have a lower porosity than the fly ash and glass powder modified pastes at intermediate ages because the effect of fly ash and glass powder is primarily of dilution at these ages. At later ages (~90 days curing), the secondary hydration of fly ash and glass powder compensates for the dilution effect, resulting in porosities similar to that of the plain paste, as shown in Fig. 2 (at the start of leaching). The silica fume modified paste shows lower porosity at the start of leaching, attributable to its higher reactivity and efficiency in densifying the material microstructure.

For a dense paste subjected to leaching, dissolution and creation of additional porosity initially occurs mainly at the leaching front. In the case of porous pastes, early dissolution can occur even at a certain depth from the surface due to the transport of leachant into the paste due to its porosity. Porosity creation in leached samples is also dependent on the specimen volume. For instance, if a larger specimen than the one used in this study is subjected to leaching, and if the m_L/m_p value is kept the same, the leaching depth will be similar to that of the smaller specimen, but the total porosity will be lower because the larger specimen will have a larger unleached core. In this paper, the influence of specimen volume on leaching is not considered, and the attempt is to compare the influence of the supplementary cementing materials in providing leaching resistance to the pastes.

From Fig. 2, it can be seen that the porosity increases with increase in leaching duration as will be expected for all the pastes. The increase in porosity resulting from leaching is seen to be the highest for the plain paste, which could be due to its higher initial CH content, which is reported to influence the rate of leaching [28]. The glass powder modified paste shows the least change in porosity with leaching. This indicates that calcium ions are being leached at a lower rate from the glass powder modified pastes as compared to the other pastes used in this study. One reason for this observation could be the higher Na_2O content of glass powder (see Table 1), which results in the production of NaOH in the pore solution, thereby reducing the dissolution of CH due to common ion effect. The addition of alkali hydroxides to a solvent is reported to significantly reduce the solubility of CH, and the reduction depends on the alkali hydroxide concentration [29]. The silica fume modified paste shows the lowest porosity in an unleached state because of higher degree of secondary hydration and denser pore structure. However, with increased leaching duration, the porosity of silica fume modified paste increases at a faster rate than for fly ash and glass powder modified pastes. The reason for this observation is given in a later section (Section 3.3.1) using the CH and C–S–H contents in the unleached and leached specimens.

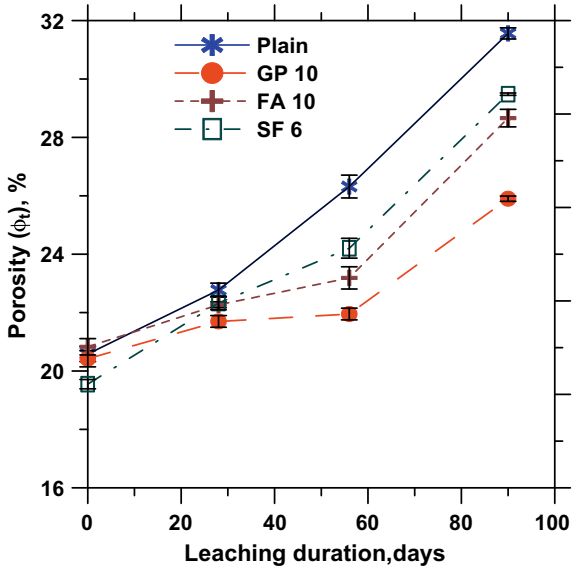

Fig. 2. Total porosity of cement pastes as a function of the leaching duration (specimens cured for 90 days before leaching).

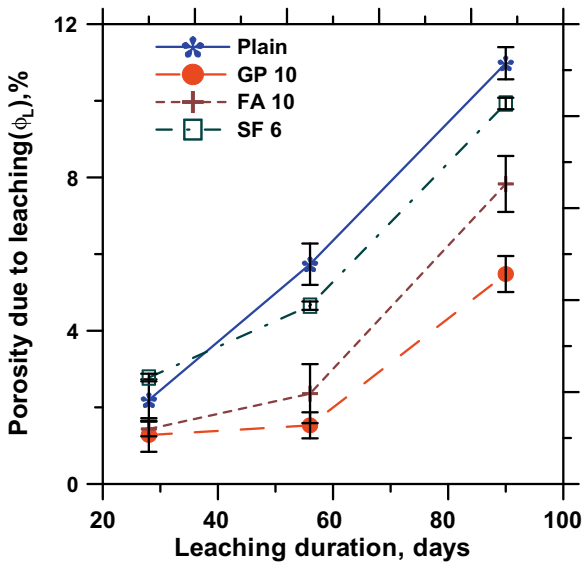

Fig. 3. Increase in porosity of cement pastes due to leaching as a function of leaching duration.

Fig. 3 shows the difference in porosities (ϕ_L) between the unleached specimen and those leached for a particular duration, as a function of leaching duration for all the pastes. C–S–H decalcification also occurs, in addition to the predominant CH leaching, when the CH is locally depleted and there is a temporary reduction in the local Ca–Si molar ratio as a large amount of Ca ions dissolves from the surface layer. The values of ϕ_L shown in Fig. 3 include the porosities created by Ca ion leaching from both C–S–H (ϕ_{CSH}) and CH (ϕ_{CH}), as shown in Eq. (3).

$$\phi_L = \phi_{CH} + \phi_{CSH} \tag{3}$$

The relative diffusion coefficient (D_e/D_o) of any species in an unleached cementitious matrix can be related to the porosity (ϕ) as [30]:

$$\frac{D_e}{D_o} = 0.001 + 0.07\phi^2 + H(\phi - 0.18) * 1.8 * (\phi - 0.18)^2 \tag{4}$$

where D_e is the effective diffusion coefficient, H(x) the Heaviside function (0 when $x \leqslant 0$, and 1 when $x > 0$), and D_o is the molecular diffusion coefficient (0.8×10^{-9} m^2/s in pure water) [14,31]. The value of 0.18 corresponds to the percolation threshold of porosity in cement pastes. This equation was developed considering the dependence of cement paste diffusivity on the pore structure. The diffusivity is dominated by the capillary pore space when the paste porosity is greater than the percolation threshold (i.e., $\phi > 0.18$), and by the continuously connected C–S–H gel pores when the capillary pore space is depercolated. The development of Eq. (4) considers pure capillary pore space diffusivity above $\phi = 0.18$, and a combination of capillary pore space and C–S–H pathways to be roughly in parallel for all values of ϕ [30].

However, Eq. (4) is not valid for leached specimens because the diffusivity increases much more rapidly when leached in comparison to its decrease due to hydration. Using a reduced percolation threshold of 0.16, a modified equation for the relative diffusion coefficient is provided in [17] for leached specimens as given below. The modification of Eq. (4) is carried out in [32] based on relative diffusion coefficients predicted by the NIST microstructural model.

$$\frac{D_e}{D_o} = 0.001 - 0.07\phi^2 + H(\phi_T - 0.16) * 3.6 * (\phi_T - 0.16)^2 - H(\phi - 0.18) * 1.8 * (\phi - 0.18)^2 + 0.14\phi_T^2 \tag{5}$$

Here, ϕ_T is the porosity of the leached specimens, which is equal to $\phi + \phi_L$.

Fig. 4 shows the relationship between the total porosity (ϕ_T) and the effective diffusion coefficient (D_e) calculated using Eq. (5) for the specimens leached in deionized water for different durations. The effective diffusion coefficient increases with increase in porosity, and the relationship is exponential. A similar exponential relationship has been observed in [3], where as the diffusion coefficients were related to the square of the porosity in [11].

3.2. Calcium hydroxide contents

Fig. 5 shows the CH contents remaining in the unleached cement pastes as well as after 28 and 90 days of leaching in deionized water, determined from thermogravimetric analysis. The CH contents in the specimens are seen to decrease rapidly for the first 28 days because there is a higher concentration gradient between the pore solution and the leachant (pure deionized water initially). The rate of leaching of Ca ions from CH is seen to slow down after 28 days because of the lower difference in concentration gradients – the CH contents in the specimens decrease, and those in the leachant increase, due to leaching. In this study, the leachant was not renewed during the test, but renewing the deionized water often can be expected to accelerate the rate of leaching until all the CH is dissolved. The plain paste suffers the maximum CH loss during 90 days of leaching. The glass powder and fly ash modified pastes show reduced loss of CH than the plain paste, indicating higher leaching resistance for these modified mixtures. The silica fume modified paste shows the lowest CH content after leaching among the modified pastes, attributable to its lower initial CH content because of the increased secondary hydration of silica fume.

3.3. Separation of porosities created due to Ca ion leaching from CH and C–S–H

An approach is detailed in this section to separate the contributions of CH and C–S–H dissolution towards the increase in porosity of cement pastes. The volume fractions of CH and C–S–H leached determined indirectly from thermal analysis are used along with the measured increase in porosity (ϕ_L) shown in Fig. 3 to separate the porosities attributable to CH and C–S–H dissolution.

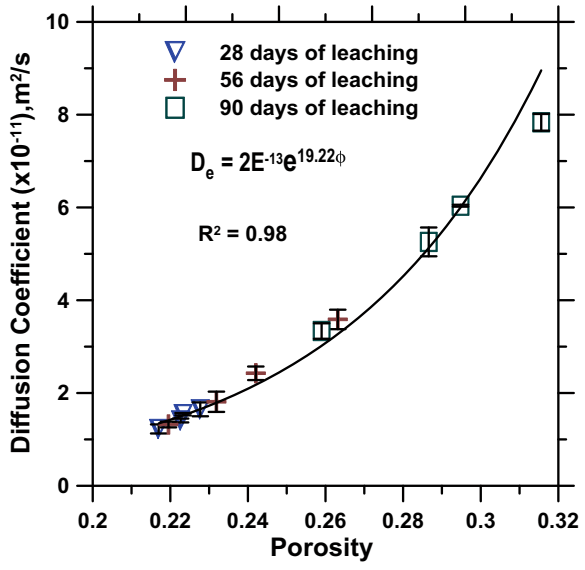

Fig. 4. Relationship between effective diffusion coefficient and porosity for cement pastes subjected to leaching.

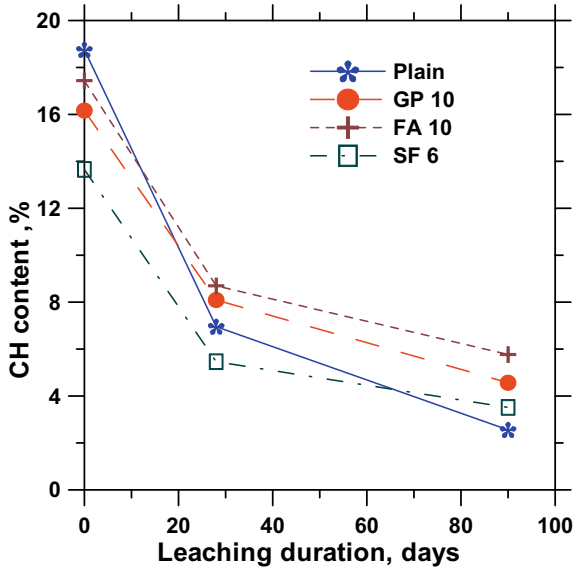

Fig. 5. Calcium hydroxide contents in the pastes before and after leaching in deionized water.

3.3.1. Volumes of CH and C–S–H leached as fractions of their respective volumes in unleached specimen

For leached specimens, thermal analysis was carried out on a representative volume of the sample from the specimen edge that incorporated a sound portion and leached zones (Fig. 1). Eq. (1) was used to calculate the mass percentages of CH in the unleached and leached pastes. These values were converted into volume percentages of CH in the unleached and leached specimens using the density of CH (2.24 g/cc) [11]. The volume of CH leached as a fraction of total CH content in the unleached specimen (Δv_{CH}) can then be expressed as:

$$\Delta v_{CH} = \frac{(V_{CH})_{\text{unleached-paste}} - (V_{CH})_{\text{leached-paste}}}{(V_{CH})_{\text{unleached-paste}}} \tag{6}$$

where $(V_{CH})_{\text{unleached-paste}}$ and $(V_{CH})_{\text{leached-paste}}$ are the volume percentages of CH in the unleached and leached specimens, respectively.

The calculation of the volume of C–S–H leached is not as straightforward because, when leaching from C–S–H is considered, it is mainly decalcification that occurs, leaving behind a silica gel in the matrix. The porosity created when leaching from C–S–H occurs is assumed to be equal to the removal of an equivalent volume of CH from C–S–H gel, as proposed in [6], i.e., a one-to-one correspondence could be assumed between the CH leached from C–S–H and the porosity created due to this leaching.

The volume of CH leached from C–S–H as a fraction of the total C–S–H content in the specimen [$(\Delta v_{CH})_{CSH}$] is therefore determined as:

$$(\Delta v_{CH})_{CSH} = \left(\frac{(V_{CH})_{C-S-H}}{(V_{CSH})_{\text{unleached-paste}}} \right) \tag{7}$$

$(V_{CH})_{C-S-H}$ is the volume of CH leached from C–S–H, which can determined by dividing the mass of C–S–H leached (the difference in the masses of C–S–H in the unleached and leached specimens determined from thermal analysis) by the density of CH. $(V_{CSH})_{\text{unleached-paste}}$ is the volume of C–S–H in the unleached paste.

Fig. 6a and b show the CH and C–S–H volume fractions leached, respectively, after 28 and 90 days of leaching. From Fig. 6a, it can be seen that the CH volume fraction leached is the highest for the plain paste, in line with the thermal analysis results shown in Fig. 5. With increasing leaching duration, the CH volume fraction leached increases for all the pastes. The silica fume modified paste shows higher volume fractions of CH leached than the other modified pastes. The reason for this could be the lower volume of $(V_{CH})_{\text{unleached-paste}}$ for the silica fume modified paste because of its increased secondary hydration.

The volume fractions of C–S–H leached (or, the CH from C–S–H, to be more precise) shown in Fig. 6b are always much lower than the volume fractions of CH leached, showing that in all the pastes studied, the predominant dissolving species is CH. This is not surprising because decalcification of C–S–H occurs only when CH is inaccessible, locally depleted, or the pH of the pore solution is drastically changed due to CH dissolution [33]. No significant difference is noticed between the C–S–H fractions leached after 28 and 90 days of exposure to deionized water for fly ash and glass powder modified pastes, and these values are lower as compared to that of the plain paste. This could be attributed to the later age secondary reaction of these materials that produce additional C–S–H gel, thus replacing some of the C–S–H leached. This goes on to show that calcium leaching and microstructure development due to hydration are essentially coupled for pastes modified with moderately active secondary cementing materials, at least for the durations studied in this paper. The silica fume modified paste shows a higher loss of Ca ions from C–S–H after 90 days. Because of its lower initial CH content, the propensity to lose Ca ions from C–S–H might be higher for silica fume modified pastes. However, this does not mean that there is a net lower C–S–H content in the silica fume modified paste after leaching as compared to the plain and other modified pastes. This is quantified in a later section through the use of equilibrium concentration curves for calcium.

3.3.2. Contributions from CH and C–S–H leaching to porosity enhancement

From the volume fractions of CH and C–S–H leached [ΔV_{CH} and $(\Delta V_{CH})_{CSH}$], the volume of CH leached as a function of the total leached volume (f_{CH}) can be calculated as:

$$f_{CH} = \frac{\Delta v_{CH}}{\Delta v_{CH} + (\Delta v_{CH})_{CSH}} \tag{8}$$

The porosity created by the leaching of Ca ions from CH (ϕ_{CH}) is then determined as:

$$\phi_{CH} = f_{CH}\phi_L \tag{9a}$$

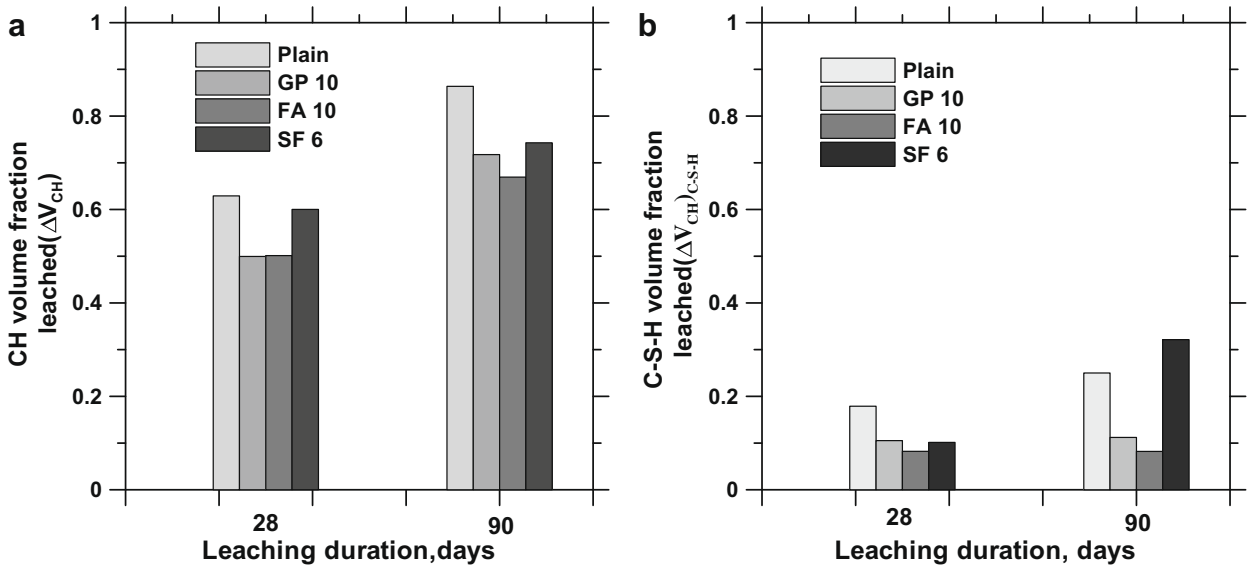

Fig. 6. Volume of: (a) CH leached as a fraction of total CH in the unleached specimen, and (b) C–S–H leached as a fraction of total C–S–H in the unleached specimen.

From Eq. (3), it follows that:

$$\phi_{CSH} = \phi_L - \phi_{CH} \quad (9b)$$

Fig. 7a and b show the porosity increase due to CH dissolution and C–S–H decalcification, respectively, determined using the procedure described above. At both the leaching durations, CH dissolution contributes to large increase in porosity. Though negligible for shorter leaching durations (28 days), porosity increase due to decalcification of C–S–H is not insignificant at longer leaching durations. The plain paste shows the largest porosity increase due to CH dissolution at later ages, while the glass powder modified paste shows the least increase because of reasons explained earlier. As far as C–S–H decalcification is concerned, the glass powder and fly ash modified pastes behave similarly, and show the least increase in porosity. Continuing secondary hydration in these pastes during the leaching duration can explain this behavior. The porosity increase due to decalcification of C–S–H is similar for the plain and the silica fume modified pastes for both the leaching durations.

3.4. Solid–liquid equilibrium curves for calcium

Leaching is a combined diffusion–dissolution process, where the cement hydrates dissociate as shown in Eqs. (10a) and (10b) [5] as a result of diffusion of ions driven by the concentration gradient between the alkaline pore solution and external deionized water. The reduction in the concentration of Ca ions in the pore solution leads to further dissolution of CH and/or C–S–H to supply Ca ions to maintain equilibrium.

$$Ca(OH)_2 \rightarrow Ca^{2+} + 2OH^- \quad (10a)$$

$$C{-}S{-}H \rightarrow Ca^{2+} + SiO_2 + 2OH^- \quad (10b)$$

The relationship between the calcium ion concentrations in the solid phases (C–S–H and CH) and in the pore solution is well known [13,20,34]. A typical solid–liquid equilibrium relationship for calcium is shown in Fig. 8. C_{CSH} is the calcium ion concentration in C–S–H gel, and C_{CH} is the calcium ion concentration in the CH phase. The use of such equilibrium relationships helps to visualize the influence of supplementary materials on the total calcium ion concentration in the C–S–H gel as well as CH, and the solubility of CH. These curves also help to quantify the influence of leaching

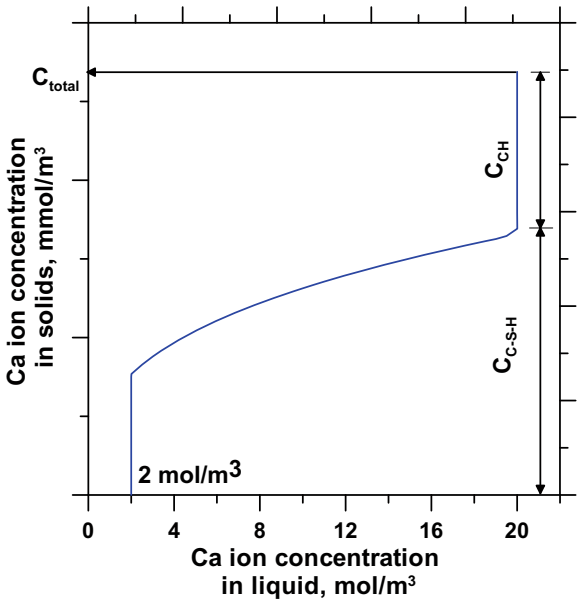

Fig. 8. A typical solid–liquid equilibrium curve for calcium.

(leachant volume, type, and leaching duration) on the amounts of Ca ions remaining in the CH and C–S–H phases of the pastes.

The dissolution of CH occurs when the Ca ion concentration in the pore solution drops below 22 mol/m^3 (mmol/l). C–S–H gels are stable between liquid Ca ion concentrations of 22 mol/m^3 and 2 mol/m^3, depending on the Ca–Si molar ratio of the gel (higher the Ca–Si molar ratio, higher the equilibrium liquid ion concentration). At Ca ion concentrations in liquid of less than 2 mol/m^3, only the silicon rich gels are stable [12,18].

In order to model the solid–liquid equilibrium relationship, this paper utilizes a model proposed in [12]. The Ca ion concentration in the solid phase (C_{solid}) is expressed as a function of the Ca ion concentration in the liquid phase (C_{liquid}) as shown below:

$$C_{Solid} = A\left[C_{CSH}\left(\frac{C_{liquid}}{C_{sat}}\right)^{\frac{1}{3}}\right] + B \quad (11)$$

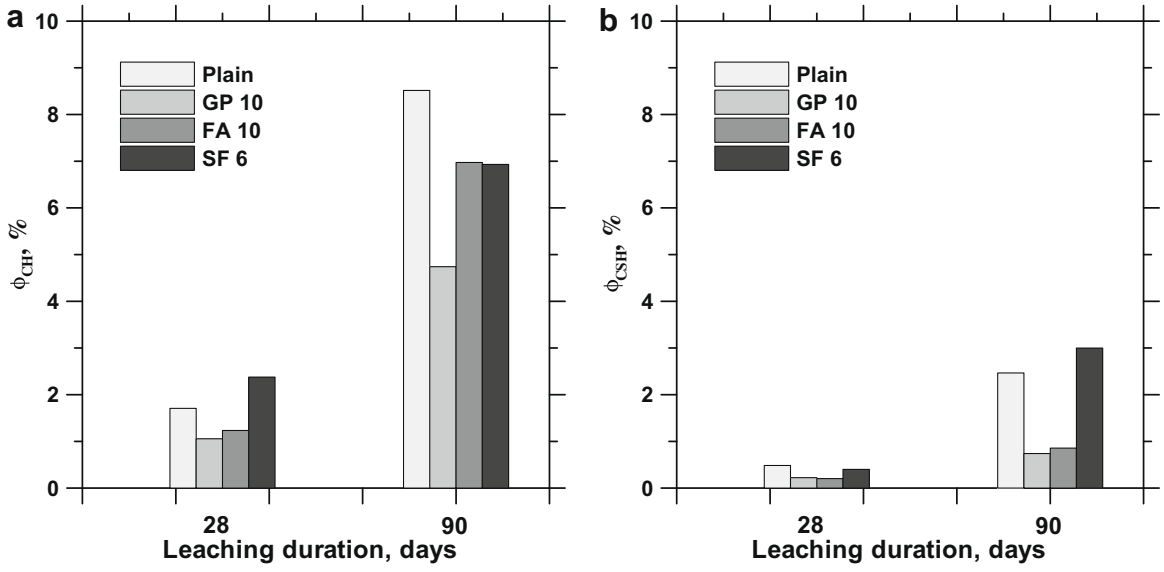

Fig. 7. Porosity created due to leaching of Ca ions from: (a) CH, and (b) C–S–H phases after 28 and 90 days of leaching.

where C_{sat} is the saturated liquid phase Ca ion concentration (mol/m^3 or mmol/l), and C_{CSH} is the calcium ion concentration in the C–S–H phase (mmol/m^3).

The constants A and B in Eq. (11) are defined as follows:

$$A = \begin{cases} -\frac{2}{x_1^3}C_{liquid}^3 + \frac{3}{x_1^2}C_{liquid}^2 & \text{for } 0 \le C_{liquid} < x_1 \\ 0 & \text{for } x_2 < C_{liquid} \end{cases} \quad (12)$$

$$B = \begin{cases} 0 & \text{for } 0 \le C_{liquid} < x_1 \\ \frac{C_{CH}}{(C_{sat}-x_2)^3}\cdot(C_{liquid}-x_2)^3 & \text{for } x_2 < C_{liquid} \end{cases} \quad (13)$$

x_1 = 2 mol/m^3, which is the Ca ion concentration in the liquid below which no C–S–H gel exists, and x_2 is the Ca ion concentration at which CH has completely dissolved. For computational ease, x_2 is taken as $(C_{sat} - 3)$ mol/m^3 [12].

3.4.1. Determination of calcium ion concentrations in CH and C–S–H phases of the unleached pastes

The model for solid–liquid equilibrium of calcium ions described above is applied in this study for the unleached pastes as well as pastes leached for 90 days in deionized water. In order to use this model, it is essential to determine the values of C_{CSH} and C_{CH}. The total calcium ion concentrations in the C–S–H and CH phases were determined from the Bogue composition of the cement, by employing the following equations [35,36] for the hydration of C_3S and C_2S.

$$C_3S + 5.3H \rightarrow C_{1.7}SH_4 + 1.3CH \quad (14a)$$

$$C_2S + 4.3H \rightarrow C_{1.7}SH_4 + 0.3CH \quad (14b)$$

To simplify the calculations, Ca ion concentrations in the aluminate hydrates were not accounted for. The amounts of C–S–H and CH per unit volume of the paste were determined stoichiometrically from Eqs. (14a) and (14b), which allows for the estimation of Ca and Si ion concentrations in the solids. As can be observed from these equations, the Ca–Si molar ratio in C–S–H gels produced from C_3S and C_2S hydration is equal to 1.7.

To calculate the amount of Ca ions in the modified pastes, the reaction of CH to produce secondary C–S–H gel shown in Eq. (15) [37] is used.

$$1.1CH + S + 2.8H \rightarrow C_{1.1}SH_{3.9} \quad (15)$$

The CH consumed in the secondary reaction of the cement replacement materials used [$(CH)_{consumed}$] were calculated using the CH contents of the plain and modified pastes determined from thermogravimetric analysis as:

$$(CH)_{consumed} = (CH)_{plain\text{-}paste}\cdot(m_{cement}) - (CH)_{modified\text{-}paste} \quad (16)$$

In Eq. (16), m_{cement} is the mass fraction of cement in the paste containing the replacement material.

The value of $(CH)_{consumed}$ was converted into moles of Ca ions per m^3 and subtracted from the Ca ion concentration (in moles/m^3) of CH produced by the cement fraction of the modified paste. Also, this amount was added to Ca ion concentration in C–S–H gel because it can be observed from Eq. (15) that 1.1 moles of CH will result in an equal amount of Ca in the secondary C–S–H gel. It can also be noticed from Eq. (15) that the Ca–Si molar ratio will decrease for all the modified pastes due to lower amount of Ca in the secondary C–S–H gel ($C_{1.1}$ for secondary hydration instead of $C_{1.7}$ for cement hydration). Higher the amount of secondary C–S–H gel produced, lower the Ca–Si molar ratio.

The Ca ion concentrations in the solid phases for completely hydrated pastes were corrected by the degrees of hydration of the respective pastes. It is well known that the quantification of cement hydration and the replacement material reaction in a paste is not straightforward because of the difficulties in separating the bound water contents associated with both the reactions. A model has been previously developed [38], where the change in non-evaporable water content of a cement paste due to the incorporation of a replacement material [$(\Delta w_n)_r$] was expressed as a function of the total measured non-evaporable water content of the paste, the non-evaporable water content of a corresponding paste with no cement replacement material, and the mass fractions of the cement and the replacement material in the paste, all of which are easily measurable experimentally. The value of $(\Delta w_n)_r$ was used along with the total measured non-evaporable water content of the paste, and the ultimate non-evaporable water contents of the plain cement and the replacement material to determine the combined degrees of hydration of the paste. This methodology does not separate the degrees of hydration of the cement and the replacement material; rather it provides the overall degree of hydration of the binder in the paste. Details on model development and its application to a few modified pastes can be found in [38]. The degrees of hydration at 90 days were determined as 0.85 for the plain paste, 0.82 for the pastes modified with fly ash and silica fume, and 0.88 for the glass powder modified paste cured in saturated limewater for 90 days using the above model.

3.4.2. Determination of calcium ion concentrations in CH and C–S–H phases of the leached pastes

For calculating the calcium ion concentrations in the solid phase of leached specimens, the following procedure is adopted in this paper. The increase in porosity (m^3/m^3 of paste) due to leaching of CH (ϕ_{CH}) and C–S–H (ϕ_{CSH}), calculated from Eqs. (9a) and (9b) were used along with the density (ρ, in kg/m^3) of CH (since even in the case of C–S–H leaching, it is actually the dissolution of CH that contributes to porosity increase) to give the mass losses (Δm, in kg/m^3) corresponding to leaching of CH from the solid phases.

$$\Delta m_{CH} = \phi_{CH}\rho_{CH} \quad (17a)$$

$$\Delta m_{CSH} = \phi_{CSH}\rho_{CH} \quad (17b)$$

These mass loss values were used to determine the concentration of Ca ions (in moles/m^3) leached from CH and C–S–H. Deducting these values from the initial amount of Ca ions in the unleached specimens gives the Ca ion concentrations in the solid phases of the leached specimen. Since only Ca ions are leached, the Ca–Si molar ratio decreases for the leached specimens.

3.4.3. Development of solid–liquid equilibrium curves for unleached and leached pastes

From the C_{CSH} and C_{CH} values determined as described above, solid–liquid equilibrium curves can be constructed for unleached and leached specimens using Eqs. (11)–(13). For plain cement pastes with a Ca–Si molar ratio of 1.7, C_{sat} (the liquid Ca ion concentration at which CH starts to dissolve) was taken as 22 mmol/l. The values of Ca–Si molar ratios for all the pastes in the unleached and leached states were calculated and are shown in Table 2. To obtain equilibrium liquid Ca ion concentrations corresponding to the Ca–Si molar ratios of the plain and modified pastes in the unleached and leached states, a thermodynamic dissolution model for C–S–H [39] that predicts the a wide range of experimental data well is used in this paper. The values of equilibrium Ca ion concentrations in the liquid for the unleached and leached states are also shown in Table 2.

For glass powder modified pastes, the higher alkali ion concentration in the pore solution will also influence the solubility of CH. Using 10% glass powder (containing 13.7% of Na_2O) as cement replacement results in a NaOH concentration of approximately 0.03 N in the pore solution. This is after taking into account the fact that only a small fraction of Na_2O in glass powder is soluble, as

Table 2
Ca–Si molar ratios and the corresponding Ca ion concentration in the liquid for unleached and leached pastes.

Paste designation	Unleached state		Leached for 90 days	
	Ca/Si	Ca ion concentration in liquid (mol/m^3)	Ca/Si	Ca ion concentration in liquid (mol/m^3)
Plain	1.70	22.0	1.51	17.0
GP 10	1.67	17.8	1.61	16.5
FA 10	1.67	21.2	1.60	19.4
SF 6	1.57	18.5	1.38	13.6

determined from flame emission spectroscopy [38]. This will reduce the liquid Ca ion saturation concentration in the unleached state from 22 mol/m^3 to 18.5 mol/m^3, based on data on CH solubility in NaOH solutions provided in [29]. Accounting for the lower Ca–Si molar ratio also (1.67 as opposed to 1.7 for plain paste), the equilibrium Ca ion concentration in the liquid phase for the glass powder modified paste is determined as 17.8 mol/m^3. Similar calculations for the leached specimen results in an equilibrium Ca ion concentration in the liquid phase for the glass powder modified paste as 16.5 mol/m^3.

Fig. 9a shows the solid–liquid equilibrium curves for the unleached pastes which were cured under saturated conditions for 90 days. Plain paste shows the highest amount of Ca ions in CH (C_{CH}), as expected. Fly ash modified paste shows a lower amount of Ca ions in C–S–H gel. The fly ash dosage (10% in this case) is not enough to produce additional C–S–H gel that can compensate for the cement dilution, though a marginal reduction in CH content is observed. Silica fume modified paste shows the least amount of Ca ions in CH and highest amount of Ca ions in C–S–H gel due to its higher degree of secondary hydration, attributable to its higher reactivity. The Ca content in C–S–H for glass powder modified pastes is slightly higher than that of the plain paste and the Ca content in CH is slightly lower. This indicates that replacement of 10% cement by glass powder compensates for the effect of cement dilution whereas fly ash at the same replacement level has a diluting effect.

Fig. 9b shows the solid–liquid equilibrium curves for the representative zone in specimens leached for 90 days in deionized water. It can be seen that more Ca ions are lost from CH than from C–S–H for all the pastes. The glass powder modified paste shows better leaching resistance than the plain and fly ash modified pastes because of the presence of alkalis which reduces the calcium ion dissolution due to common ion effect as described earlier, even though the Ca–Si molar ratio is not very different from that of the fly ash modified paste. Also the presence of alkalis in the pore solution might increase the viscosity of the pore solution, thus making it harder to diffuse out of the paste, and thus reduce leaching [40]. The silica fume modified paste has only a fewer amount of Ca ions remaining in CH, attributable to the lower initial amount of CH in this paste. This results in further leaching of Ca ions from the C–S–H phase in the silica fume paste.

Fig. 10a shows the amount of Ca ions in CH for the unleached specimens and the amount of Ca ions leached out. It can be seen that plain paste has lost a higher amount of Ca ions due to its higher initial CH content as well as its comparatively less dense microstructure. The loss of Ca ions from CH is lower in all the modified pastes as compared to the plain paste, and is the least in glass modified pastes, the reason for which have been explained earlier. Fig. 10b shows the amount of Ca ions in C–S–H for the unleached specimens and the amount of Ca ions leached out from C–S–H. The silica fume modified paste has the highest amount of Ca ions in C–S–H gel than the other pastes due to its higher degree of secondary hydration. It can be seen that fly ash and glass powder modified pastes has lost fewer Ca ions from C–S–H gel, which is in conformity with the discussions provided in this paper. The comparison between Fig. 10a and b also clearly shows that loss of Ca ions is more prominent from CH than from C–S–H.

3.5. Estimation of leaching depths

The leaching depths (L_d) were calculated in this paper using the CH contents of the unleached specimen and the CH contents in the

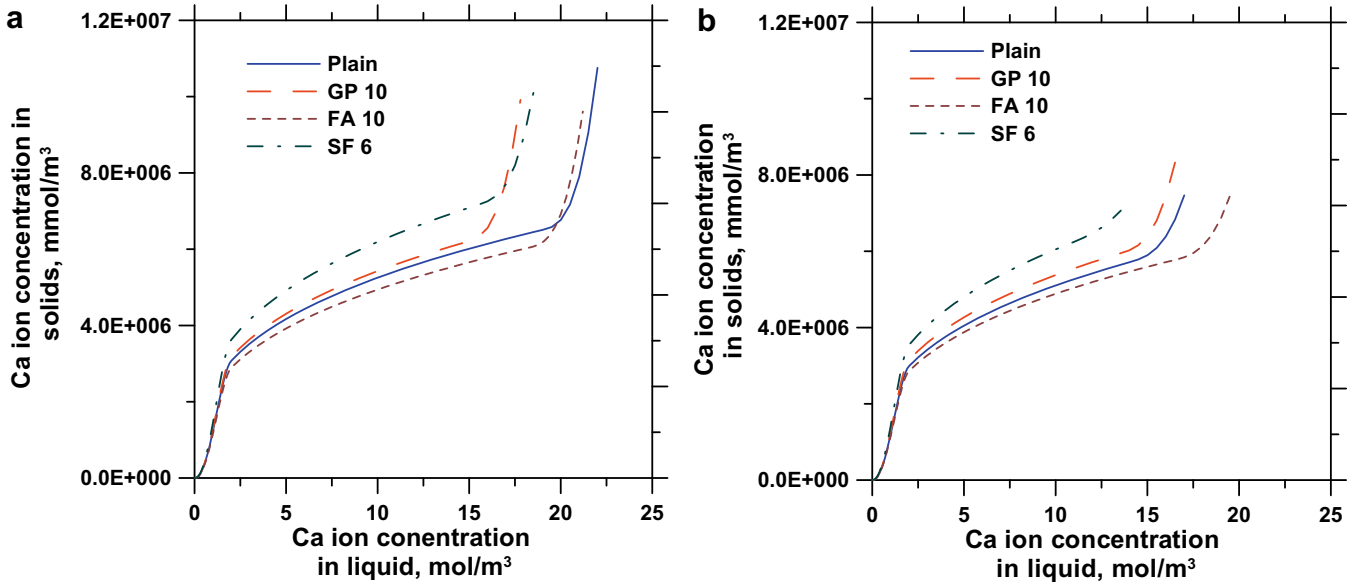

Fig. 9. Solid–liquid equilibrium curves for: (a) unleached specimens, and (b) specimens leached for 90 days.

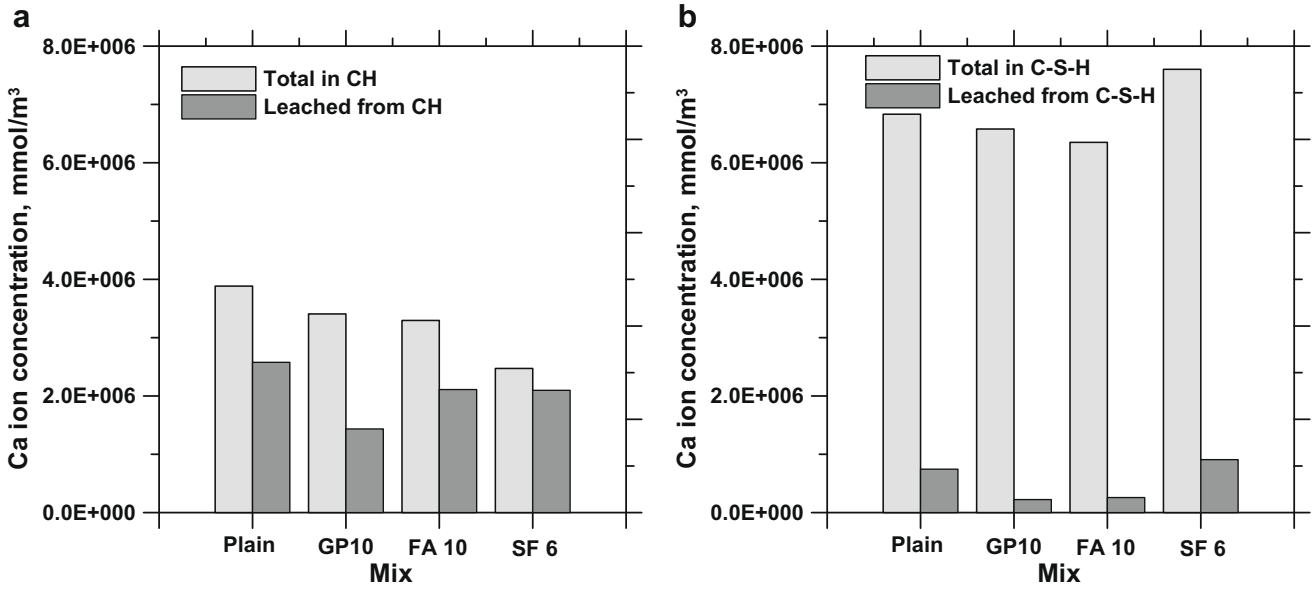

Fig. 10. Total and leached concentrations of Ca ions from: (a) CH, and (b) C–S–H phases after 90 days of leaching.

representative zone of the specimens (Fig. 1) subjected to leaching, determined from thermogravimetric analysis. The difference between the CH contents of the unleached specimen and the representative volume of the leached specimen provides the percentage CH loss due to leaching in the representative volume, which will be similar to that lost from the entire specimen. From the known volume and CH content of the unleached sample, and the CH content leached, the volume of CH lost could be determined. Dividing this by the specimen surface area gives the leaching depth (L_d).

Fig. 11 shows the leaching depths for the plain and modified pastes after 28 and 90 days of leaching. A leaching depth of 1.22 mm is obtained for the plain paste after 90 days of leaching, which is very similar to the values previously reported for similar pastes at similar leaching durations [3,41]. The leaching depths for silica fume and fly ash modified pastes are slightly lower than that of the plain paste, indicating better leaching resistance. The glass powder modified paste shows the least leaching depth at both ages indicating very good leaching resistance. The reasons explained earlier for lower Ca ion leaching from the glass powder modified paste are applicable here also.

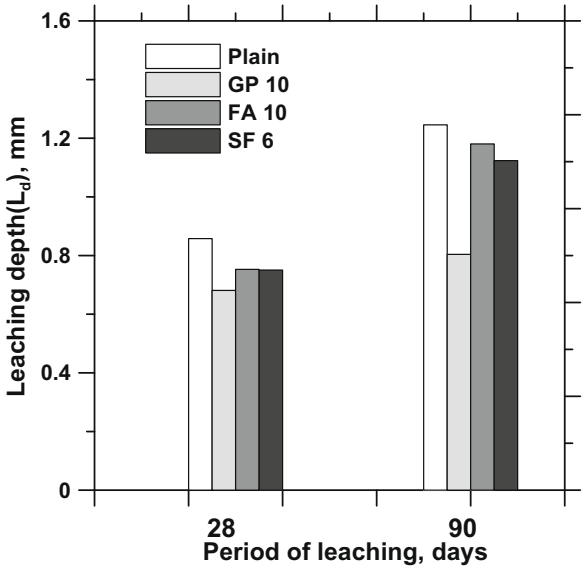

Fig. 11. Leaching depths for plain and modified pastes at different leaching durations.

4. Conclusions

This study has dealt with Ca ion leaching from cement pastes incorporating a fine glass powder, silica fume or fly ash as partial cement replacement materials. Deionized water was used as the leaching medium, and the ratio of mass of leachant to that of the solid was kept as 1000. Porosity measurements and thermogravimetric analysis, along with solid–liquid equilibrium curves for calcium ions were used to quantify the influence of the chosen dosages of the studied replacement materials on leaching, and the conclusions are presented below.

The porosity of all the cement pastes was found to increase with leaching duration, with the plain pastes showing the highest increase. The glass powder modified paste showed the lowest porosity increase, indicating higher Ca ion leaching resistance because of the presence of NaOH in its pore solution that reduces the solubility of calcium hydroxide due to the common ion effect. The total amount of Ca ions leached (and thus the total porosity created as a result of leaching) resulted from the dissociation of both the CH and C–S–H phases. The diffusion coefficients of the leached pastes were computed based on a previously published equation, using a constant value for percolation threshold (0.16), and the experimentally determined porosities. After 90 days of leaching, a lower loss of CH was observed for glass powder and fly ash modified pastes as compared to the plain paste, indicating higher leaching resistance for these modified mixtures.

This paper has also detailed an approach whereby the porosities created due to the leaching of Ca ions from the CH and C–S–H phases could be separated, using thermogravimetric data obtained from a representative specimen volume. CH dissolution has been confirmed as the main cause of porosity increase, though C–S–H decalcification also contributes to porosity enhancement, especially at longer durations of leaching. While the plain paste showed the largest porosity increase because of CH dissolution, the glass powder modified paste showed the least increase, with the other

two modified pastes in between. When porosity increase due to C–S–H decalcification was considered, the glass powder and fly ash modified pastes showed the least increase, attributable to continued secondary hydration during leaching.

Solid–liquid equilibrium curves for Ca ions were constructed for the unleached and leached cement pastes. The Ca ion concentrations of the CH and C–S–H phases of the plain pastes, which are required as inputs in the model for the equilibrium curve, were determined stoichiometrically from chemical formulae for cement hydration. For the modified pastes, these values were adjusted by the Ca ion concentrations of CH consumed and the additional low Ca–Si molar ratio C–S–H created by the secondary reaction. These equilibrium curves serve as a useful aid to visualize the amount of Ca ions in the CH and C–S–H phases before and after leaching, for plain and modified cement pastes. The CH and C–S–H contents of all the leached pastes obtained from the equilibrium curves substantiate the results from the porosity measurements. An indirect method of leaching depth determination using the CH contents of the leached and unleached specimens has also been outlined in this paper. This method provided comparable values of leaching depth as reported for similar pastes of same w/cm, and cured for similar durations.

Acknowledgements

The authors gratefully acknowledge the financial support from the Empire State Development Program of New York State towards this study. Some of the experiments reported in this paper were carried out at the facilities of the Center for Advanced Materials Processing (CAMP) at Clarkson University. The support that has facilitated the creation and maintenance of those facilities is also acknowledged.

References

[1] Adenot F, Buil M. Modeling of the corrosion of the cement paste by deionized water. Cem Concr Res 1992;22:489–96.
[2] Faucon P, Bescop PL, Adenot F, Bonville P, Jacquinot JF, Pineau F, et al. Leaching of cement paste: study of the surface layer. Cem Concr Res 1996;26(11):1707–15.
[3] Mainguy M, Tognazzi C, Torrenti JM, Adenot F. Modeling of leaching in pure cement paste and mortar. Cem Concr Res 2000;30:83–90.
[4] Kamali S, Moranville M, Leclercq S. Material and environmental parameter effects on the leaching of cement pastes: experiments and modeling. Cem Concr Res 2008;38(4):575–85.
[5] Wee TH, Zhu J, Chua HT, Wong SF. Resistance of blended cement pastes to leaching in distilled water at ambient and higher temperatures. ACI Mater J 2001;98(2):184–93.
[6] Buil M, Revertegat E, Ollivier J. A model of the attack of pure water or undersaturated lime solutions on cement. Stabilizat Solidificat Hazard, Radioact, Mixed Waste 1992;2:227–41.
[7] Kamali S, Gerard B, Moranville M. Modeling the leaching kinetics of cement based materials—influence of materials and environment. Cem Concr Compos 2003;25:451–8.
[8] Marchand J, Bentz DP, Samson E, Maltais Y. Influence of calcium hydroxide dissolution on the transport properties of hydrated cement systems. In: Workshop on the role of calcium hydroxide in concrete 2000; Holmes Beach, Anna Maria Island, Florida: p. 113–29.
[9] Carde C, Franqois R, Torrenti JM. Leaching of both calcium hydroxide and C–S–H from cement paste: modeling the mechanical behavior. Cem Concr Res 1996;26(8):1257–68.
[10] Haga K, Shibata M, Hironaga M, Tanaka S, Nagasaki S. Change in pore structure and composition of hardened cement paste during the process of dissolution. Cem Concr Res 2005;35:943–50.
[11] Haga K, Sutou S, Hironaga M, Tanaka S, Nagasaki S. Effects of porosity on leaching of Ca from hardened ordinary Portland cement paste. Cem Concr Res 2005;35:1764–75.
[12] Nakarai K, Ishida T, Maekawa K. Modeling of calcium leaching from cement hydrates couples with micro-pore solution formation. J Adv Concr Technol 2006;4(3):395–407.
[13] Mainguy M, Coussy O. Propagation fronts during calcium leaching and chloride penetration. J Eng Mech 2000;126(3):250–7.
[14] Sugiyama T, Ritthichauy W, Tsuji Y. Simultaneous transport of chloride and calcium ions in hydrated cement systems. J Adv Concr Technol 2003;1(2):127–38.
[15] Bernard F, Kamali-Bernard S, Prince W. 3D modeling of mechanical behavior of sound and leached mortar. Cem Concr Res 2008;38(4):449–58.
[16] Matte V, Moranville M. Durability of reactive powder composites: influence of silica fume on the leaching properties of very low water/binder pastes. Cem Concr Compos 1999;21(1):1–9.
[17] van Eijk RJ, Brouwers HJH. Study of the relation between hydrated portland cement composition and leaching resistance. Cem Concr Res 1998;28(6):815–28.
[18] Gaitero JJ, Campillo I, Guerrero A. Reduction of calcium leaching ratio of cement paste by addition of silica nanoparticles. Cem Concr Res 2008;38:1112–8.
[19] Haga K, Shibata M, Hironaga M, Tanaka S, Nagasaki S. Silicate anion structural change in calcium silicate hydrate gel on dissolution of hydrated cement. J Nucl Sci Technol 2002;39(5):504–47.
[20] Delagrave A, Gerard B, Marchand J. Modeling the calcium leaching mechanisms in hydrated cement paste. In: Scrivener KL, and Young JF, Editors. proceedings of the material research society's symposium on mechanisms of chemical degradation of cement-based systems, Boston, USA, November 1995. p. 38–48.
[21] Heukamp FH, Ulm FJ, Germaine JT. Poroplastic properties of calcium-leached cement-based materials. Cem Concr Res 2003;33:1155–73.
[22] Taylor HFW. Cem chemistry. London: Thomas Telford; 1997.
[23] Reardon EJ. An ion interaction model for the determination of chemical equilibria in cement/water systems. Cem Concr Res 1990;20:175–92.
[24] Rahman MM, Nagasaki S, Tanaka S. A model for dissolution of $CaO–SiO_2–H_2O$ gel at Ca/Si > 1 – For application to blended cement. Cem Concr Res 1999;29(7):1091–7.
[25] RILEM CPC11.3. Absorption of water by immersion under vacuum. Mater Struct 1984;17:391–4.
[26] Ruiz LA, Platret G, Massieu E, Ehrlacher A. The use of thermal analysis in assessing the effect of temperature on a cement paste. Cem Concr Res 2005;35:609–13.
[27] Odelson JB, Kerr EA, Vadakan WV. Young's modulus of cement paste at elevated temperatures. Cem Concr Res 2007;37:258–63.
[28] Carde C, Francois R, Ollivier JP. Microstructural changes and mechanical effects due to the leaching of calcium hydroxide from cement paste. In: Scrivener KL, and Young JF (Ed.), In: Proceedings of the material research society's symposium on mechanisms of chemical degradation of cement-based systems. Boston, USA, 27–30 November 1995. p. 30–7.
[29] Duchesne J, Reardon EJ. Measurement and prediction of portlandite solubility in alkali solutions. Cem Concr Res 1995;25(5):1043–53.
[30] Garboczi EJ, Bentz DP. Computer simulation of the diffusivity of cement based materials. J Mater Sci 1992;27:2083–92.
[31] Lagerblad B. Leaching performance of concrete based on studies of samples from old concrete constructions. Technical Report TR-01-27 2001; Swedish Nuclear Fuel and Waste Management Co Stockholm, Sweden. p. 80.
[32] Snyder KA, Clifton JR. 4sight manual: a computer program for modeling degradation of underground low level water concrete vaults. NISTIR 5612. US Department of Commerce; 1995. p. 76.
[33] Chen JJ, Thomas JJ, Jennings HM. Decalcification shrinkage of cement paste. Cem Concr Res 2006;36:30–8.
[34] Berner UR. Modeling of incongruent dissolution of hydrated cement minerals. Radiochim Acta 1988;44/45:387–93.
[35] Mounanga P, Khelidj A, Loukili A, Baroghel-Bouny V. Predicting $Ca(OH)_2$ content and chemical shrinkage of hydrating cement pastes using analytical approach. Cem Concr Res 2004;34(2):255–65.
[36] Garboczi EJ, Bentz DP, Snyder KA, Martys NS, Stutzman PE, Ferraris CF, Bullard JW. An electronic monograph: modeling the structure and properties of cement-based materials. <http://ciks.cbt.nist.gov/~bentz/chapter/section4.html>.
[37] Bentz DP, Jensen OM, Coats AM, Glasser FP. Influence of silica fume on diffusivity in cement-based materials I. Experimental and computer modeling studies on cement pastes. Cem Concr Res 2000;30:953–62.
[38] Schwarz N, Neithalath N. Influence of a fine glass powder on cement hydration: Comparison to fly ash and modeling the degree of hydration. Cem Concr Res 2008;38:429–36.
[39] Sugiyama D, Fujita T. A thermodynamic model of dissolution and precipitation of calcium silicate hydrates. Cem Concr Res 2006;36:227–37.
[40] Powers TC. Physical properties of cement paste. In: Proceedings of the fourth international symposium on chemistry of cement, Washington DC, vol. 2. 1960; p. 577–609.
[41] Moranville M, Kamali S, Guillon E. Physicochemical equilibria of cement-based materials in aggressive environments-experiments and modeling. Cem Concr Res 2004;34(9):1569–78.